EUROPEAN ORGANIZATION FOR NUCLEAR RESEARCH
ORGANISATION EUROPEENNE POUR LA RECHERCHE NUCLEAIRE

CERN - PS DIVISION

PS/ CA/ Note 99-12

SWEEPING MAGNET FOR THE TIME OF FLIGHT FACILITY AT THE CERN PS

M. Giovannozzi, M. Sassowsky

In this Note a solution for the sweeping magnet to be used in the context of the proposed Time of Flight Facility at the CERN PS is discussed. Starting from the neutron beam line geometry, the required dipolar magnetic field needed to deflect charged particles outside the beam line acceptance is worked out. Different options to design and electromagnetic device meeting the necessary specifications are then described. Finally the implementation of such a device is discussed in details.

Geneva, Switzerland
4 May 1999

1 Introduction

In the context of the proposed Time Of Flight Facility at the CERN PS [1, 2], the neutron beam, produced by a spallation process induced by the primary proton beam hitting on a lead target, needs to be separated from the charged secondary particles.

The natural choice consists in using a dipole magnet to sweep the charged particles that contaminates the neutron beam. In Ref. [2] it has been proposed to use a device based on permanent magnet technology. The main advantage of such a choice is the conceptual simplicity and the fact that no power converter is needed. This last point is particularly appealing in a situation such as that existing in the TT2A tunnel, where no infrastructure is present and the high radiation level would be in favour of a reduction of critical parts which could break down (as is the case for a power converter). However, a number of drawbacks have to be taken into account, mainly the high cost of such a device.

Therefore, the decision has been taken to study the details of a solution based on a classical, electromagnetic device.

2 General characteristics of the sweeping magnet

The schematic view of the TOF tube installed in the TT2A tunnel is shown in Fig. 1: the diameter of the vacuum pipe is decreased from the initial value of 0.8 m just downstream of the lead target to the minimum value of 0.4 m. At the location where the diameter of the vacuum pipe is reduced, concrete blocks are installed to collimate the neutron beam.

The angular acceptance of the beam line can be computed under the assumption that the decays in flight of the charged particles generated by the spallation process can be neglected. Using this hypothesis, the geometry of the beam line allows to estimate the maximum angle $\theta_{\max}$ of a charged particle reaching the sweeping magnet located L meters from the beginning of the line, namely

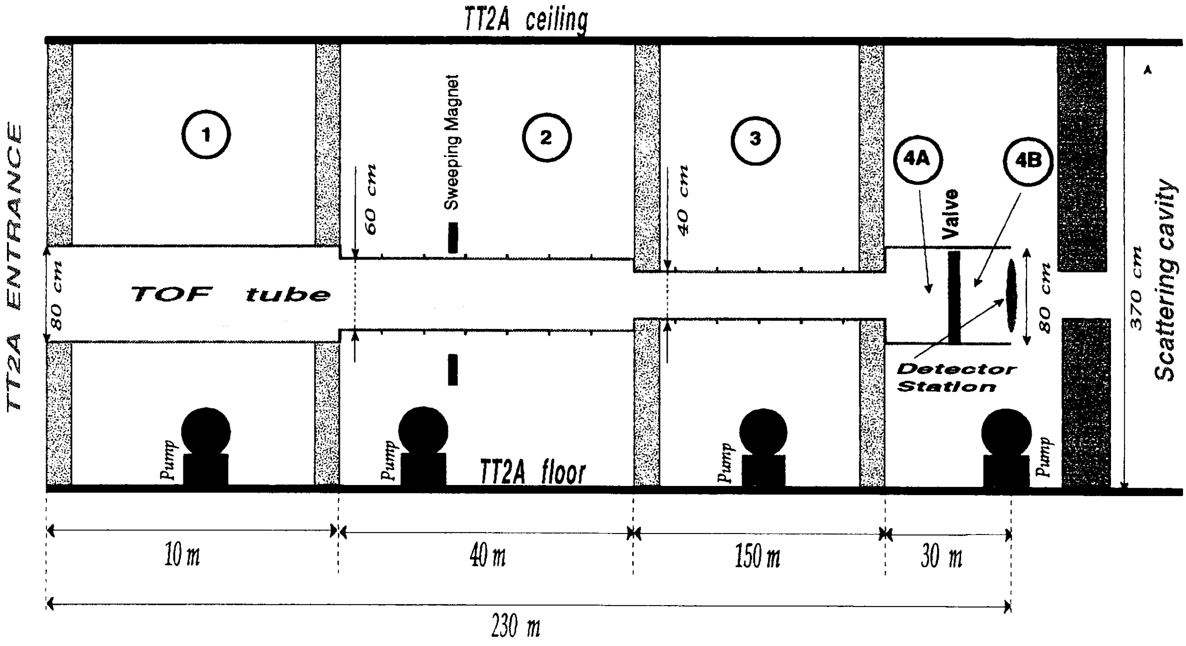

Figure 1: Layout of the Time Of Flight tube.

$$\vartheta_{\max} \approx \frac{d_{\mathrm{i}} + d_{\mathrm{mag}}}{2L}, \tag{1}$$

where d_{i} represents the diameter of the beam pipe at the entrance of the beam line and d_{mag} the diameter at the magnet location.

Furthermore, a deflection angle given by

$$\theta_{\mathrm{mag}} \approx \frac{d_{\mathrm{mag}}}{(\ell - L)}, \tag{2}$$

would allow to deflect charged particles parallel to the axis of the beam pipe so that they will hit the walls of the pipe $(\ell - L)$ meters downstream of the sweeping magnet. Hence the maximum deflection to be produced by the magnet should be given by

$$\theta_{\mathrm{max}} \approx \frac{(\ell - L)d_{\mathrm{i}} + (\ell + L)d_{\mathrm{mag}}}{2L(\ell - L)}. \tag{3}$$

Neither the position L of the sweeping magnet nor the parameter ℓ can be chosen freely, some constraints being imposed by the presence of an intermediate measuring station at about 80 m from the entry point of the beam line. This station has to be located downstream of the sweeping magnet so that the charged particles deflected by the magnet do not introduce a strong background. Realistic values of the parameters L and ℓ are 50 m and 65 m respectively. Then one obtains

$$\theta_{\mathrm{max}} = 38.7\mathrm{mrad}. \tag{4}$$

To determine the actual strength of the required magnetic field, it is necessary to evaluate the maximum momentum p_{max} of the charged particles to be deflected. In Fig. 2 the charged particle distribution as a function of energy is shown for three different products of the interaction between the proton beam and the lead target [3]. All three distributions show a rather sharp fall for a value of p of about 10 GeV/c. Therefore, it has been decided to place the cut-off at the value $p_{\mathrm{max}} = 10$ GeV/c. From this, one obtains the integrated magnetic field of the sweeping magnet, namely

$$(B\,l)_{\mathrm{max}} = \theta_{\mathrm{max}}(B\,\rho)_{\mathrm{max}} = 1.29\,\mathrm{T\,m}. \tag{5}$$

As a remark, an hypothetic secondary particle having a kinetic momentum of 24 GeV/c would reach the pipe walls about 100 m downstream the sweeping magnet under the effect of the computed angular kick $(B\,l)_{\mathrm{max}}$.

In principle, the length of the sweeping magnet can be used as a free parameter in order to reduce the absolute value of the magnetic field needed to deflect the charged particles present in the neutron beam. This opens up the possibility of using a permanent magnet to design the sweeping magnet. In recent years, there has been a considerable interest in the permanent magnet technology, also outside the usual fields of application, like undulators and other devices with a rapidly varying field configuration. As an example, one can mention the new recycler ring built at Fermilab [4]. For this reason, it was decided to explore the possibility of building a permanent magnet.

In the case of the TOF Facility, the need of a cheap and robust device, without much concern for the homogeneity of the magnetic field produced, seemed to be the ideal application for a permanent magnet. Furthermore, the absence of devices like power converters and cooling system, was very appealing in view of a reduction of the installation costs. In Fig. 3 (upper part) it is shown a possible geometry for such a device [5]. The layout is derived from that used for the Fermilab machine [4]. In the same figure (centre and lower part) the field lines are plotted for two different configurations, namely with and without shims on the pole face. As already mentioned, there are also some drawbacks in the use of a permanent magnet. First of all, the

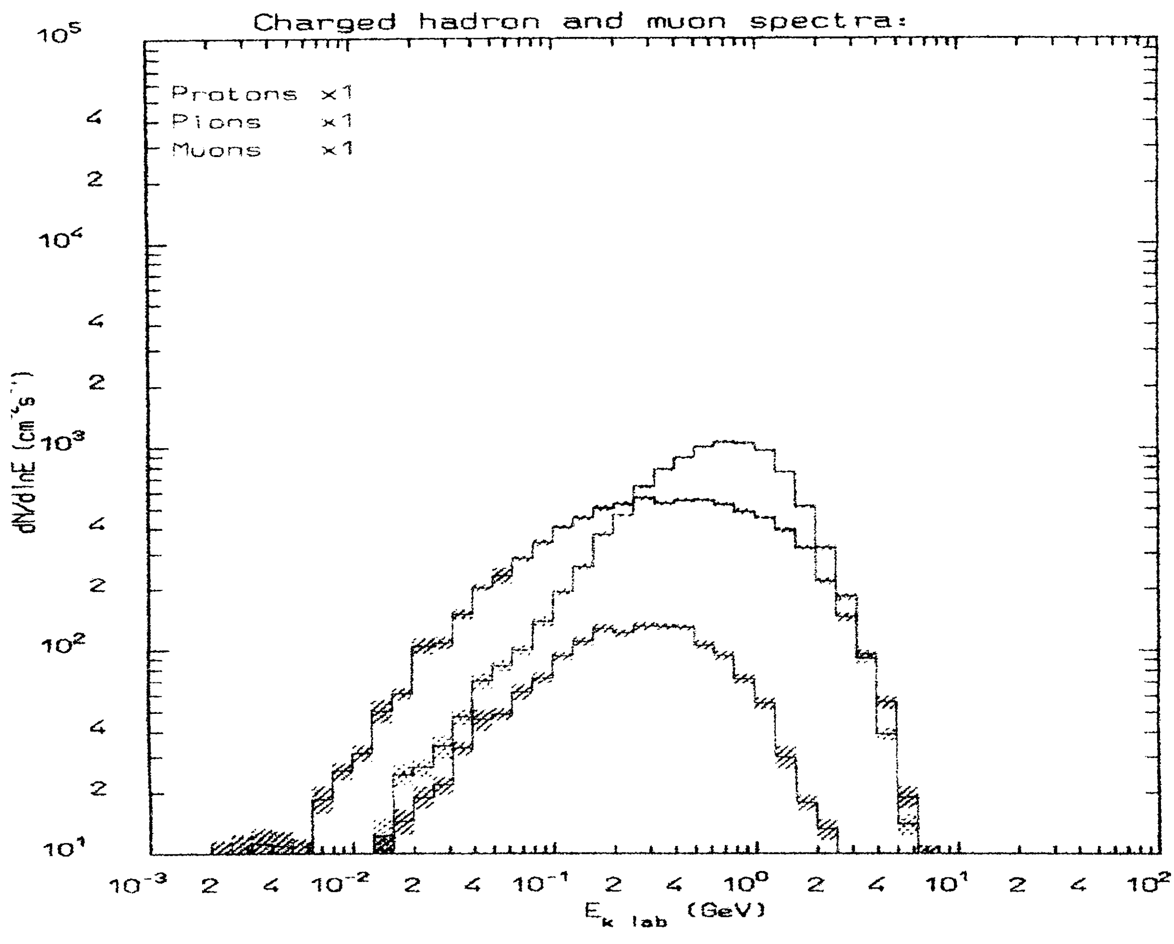

Figure 2: Distribution of the charged secondary particles produced by the spallation process as a function of energy.

radiation hardness of the permanent magnet material is a source of concern. Secondly, the price of such a device would be rather high (of the order of 120K USD). This is mainly due to the fact that CERN does not have any specific experience in building permanent magnets (thus imposing the intervention of an outside firm for the construction and, eventually, also for the design) and to the impossibility of reducing the cost via a series production (the magnet will remain at the prototype level with the related high costs). For these reasons, the solution based on the more standard approach of an electromagnetic device has been considered.

3 Simulation of the performances of an electromagnetic sweeping magnet

To reduce the costs, the approach has been to look for a suitable magnet among those available in the CERN stock. The best candidate is the M200-type magnet [6]. This is a 2 meters long magnet with a variable height gap. The gap size can be changed by varying the width of a special spacing plate installed in the iron yoke (see Fig. 4, the spacing plate is clearly visible on the left side of the magnet yoke). This would allow to increase the gap up to 410 mm by simply inserting a specially designed ARMCO spacing plate 300 mm thick. This magnet exists in two versions: with straight poles or tapered poles. In order to have enough room to install the vacuum pipe inside the yoke, it has been decided to use the straight pole type.

As far as the magnetic field is concerned, the maximum integrated field is about 3.63 T m. A simulation of the magnetic performance of this type of magnet has been carried out by using the OPERA program. In Fig. 5 it is shown the mechanical layout (upper part) together with the

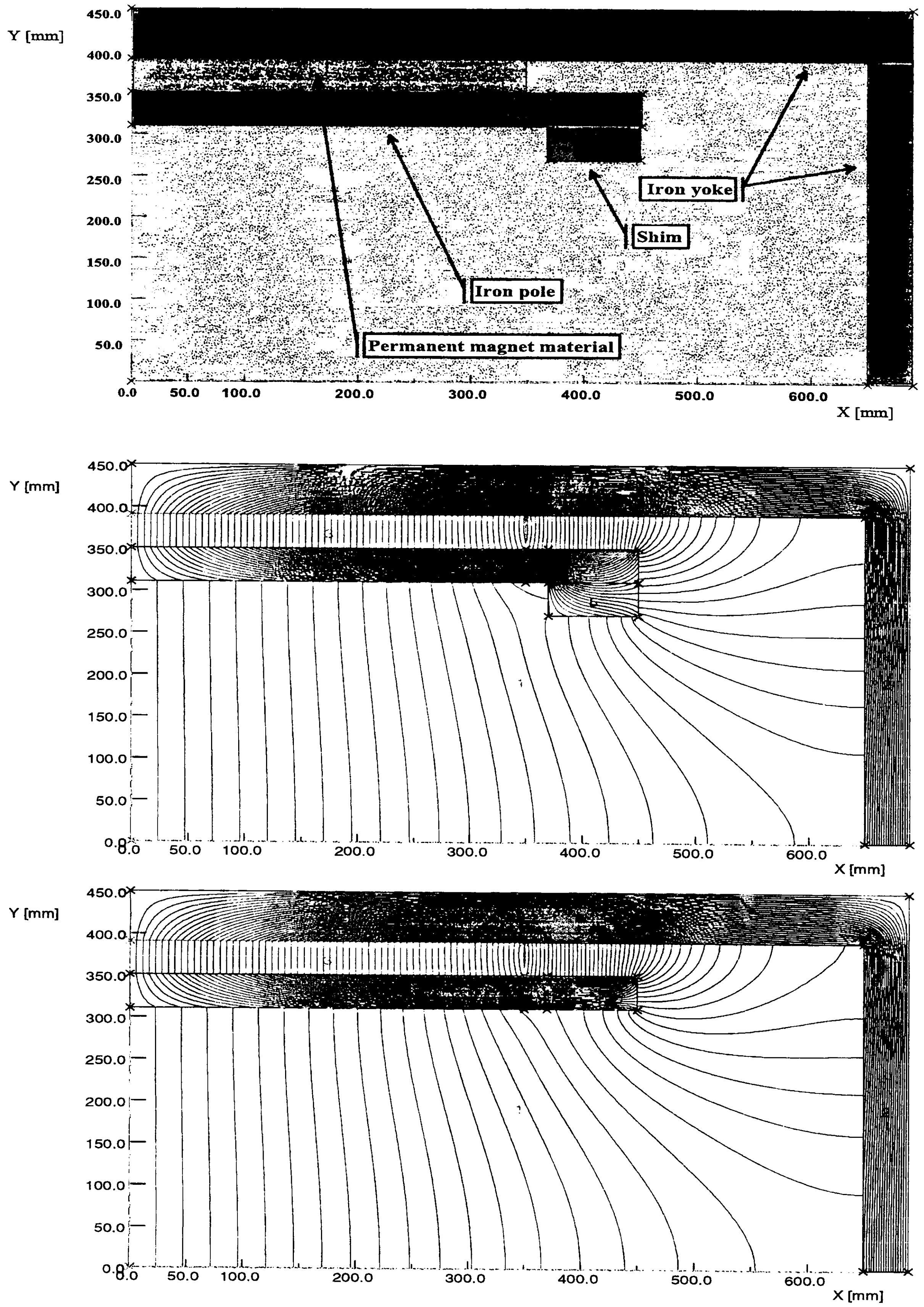

Figure 3: Different geometries for the permanent magnet solution. The general layout is shown in the upper part. In the centre and lower part the field lines for the configuration with and without shims are presented.

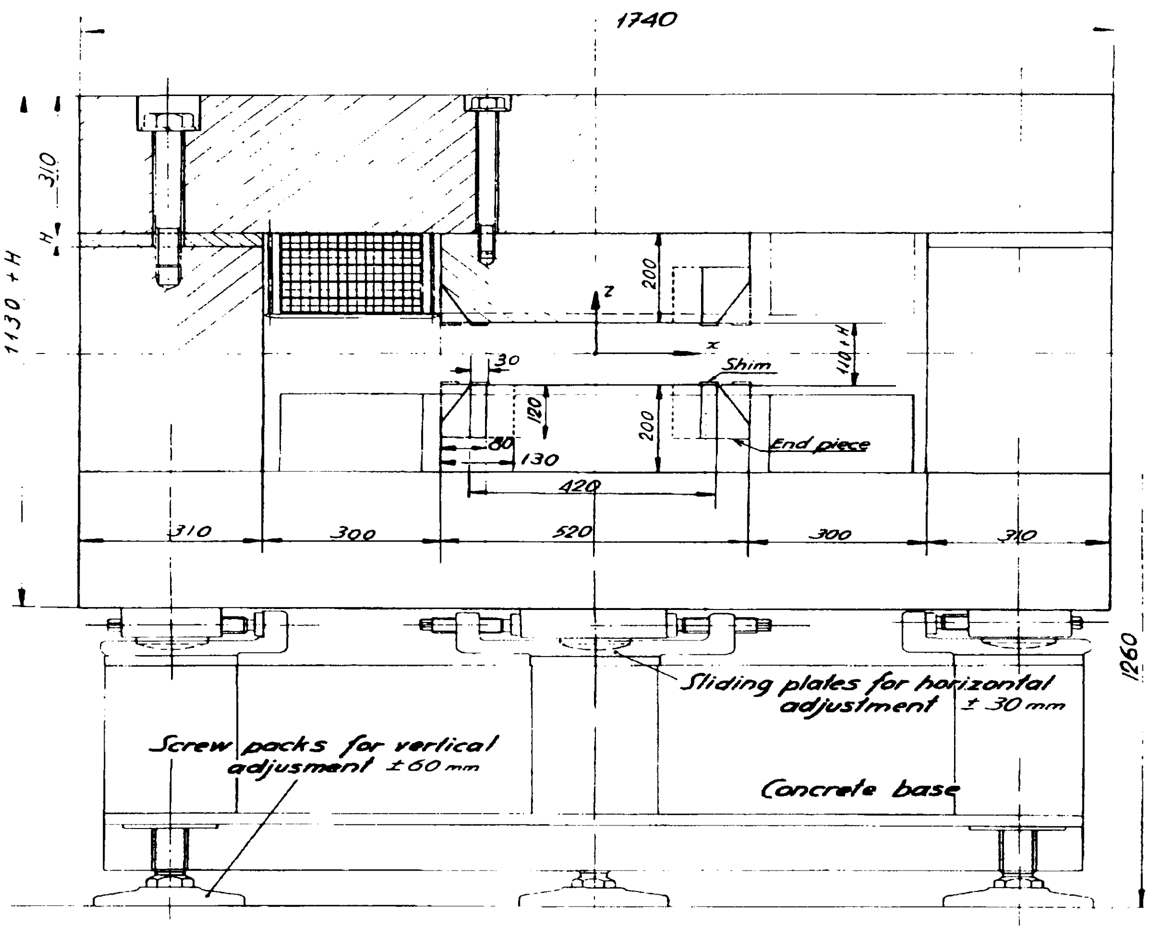

Figure 4: Mechanical layout of the M200-type magnet to be used as sweeping magnet for the TOF Facility.

field map (centre part) and the homogeneity with respect to the peak field value of 1.77 T (lower part): the field drop in the transverse direction at the pole end is about 5 %. This result allows to estimate the accuracy of the simulation. The measured peak field is 1.73 T and this value agrees with the result of the numerical simulations within 2 %. Therefore, one can be confident that the model used is capable of correctly simulating also the situation with an increased gap size.

The main parameters of the M200-type magnet, in the standard configurations, are summarised in the Table 1.

The increase in the gap size will result in a drop of the magnetic field produced which is approximately proportional to the ratio of the two gap sizes. Therefore, it is expected to have an overall reduction by a factor of three with respect to the nominal layout (140 mm gap size). This trend is confirmed by the numerical simulations shown in Fig.6: in the upper part the distribution of the field lines is plotted in the transverse plane. In the centre part the field homogeneity is shown in the form of contour plot, while in the lower plot it is reported the field homogeneity as a function of the transverse coordinate. The peak field reaches a value of 0.75 T, thus giving an integrated field of about 1.5 T m. This is a rather conservative estimate, as the magnetic length will be bigger than the mechanical length of the magnet, due to the very large gap size. The field homogeneity is about 10 %, but this is not a major source of concern in this specific case. In fact, the field quality is not relevant as long as the minimum integrated field is high enough to deflect the charged particles and this is certainly the case for the field drop obtained

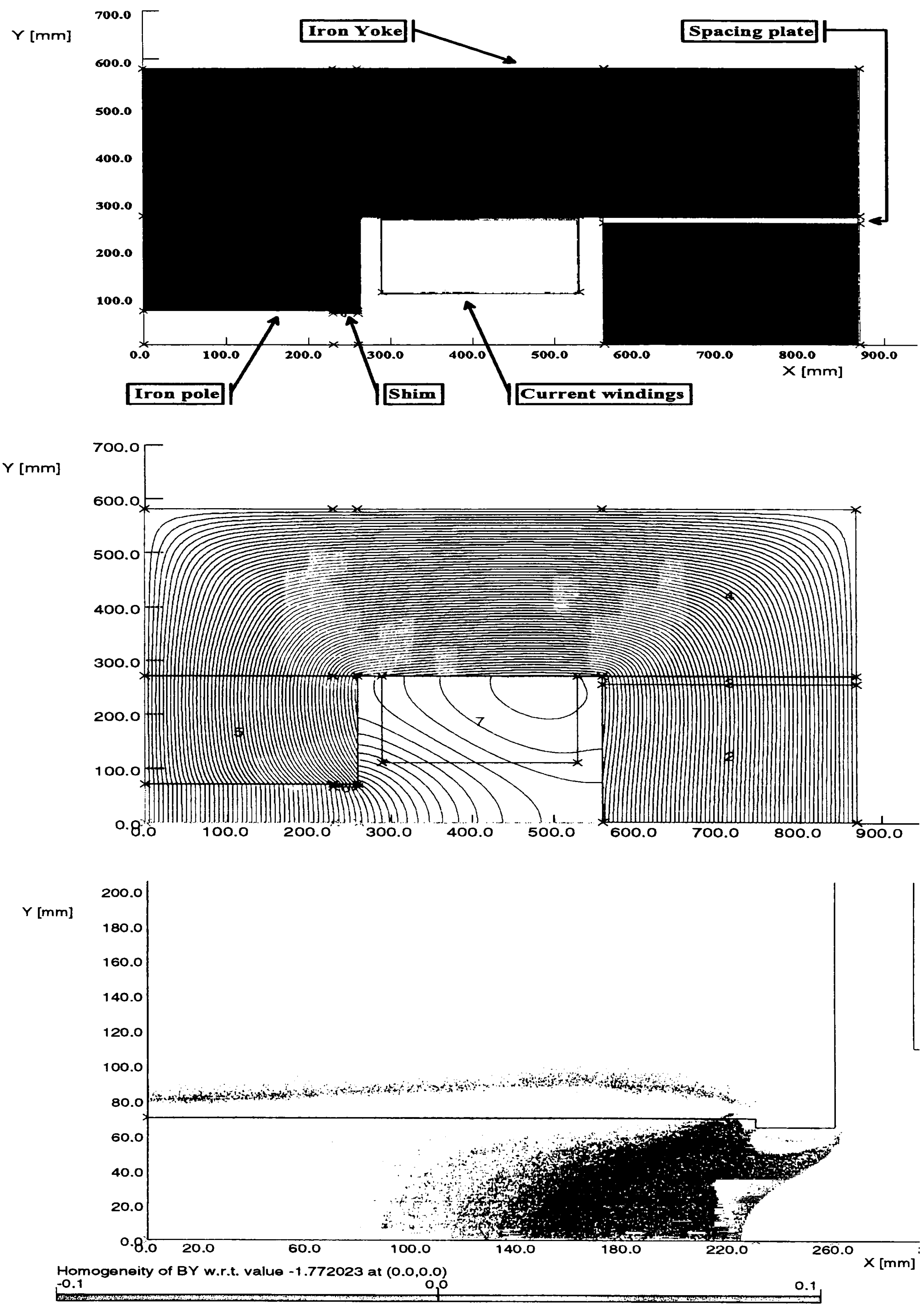

Figure 5: Layout of the M200-type magnet to be used as sweeping magnet for the TOF Facility. The geometry is shown in the upper part. In the centre part the field map is shown for the standard configuration (140 mm gap), while in the lower part the field homogeneity with respect to the peak value is shown.

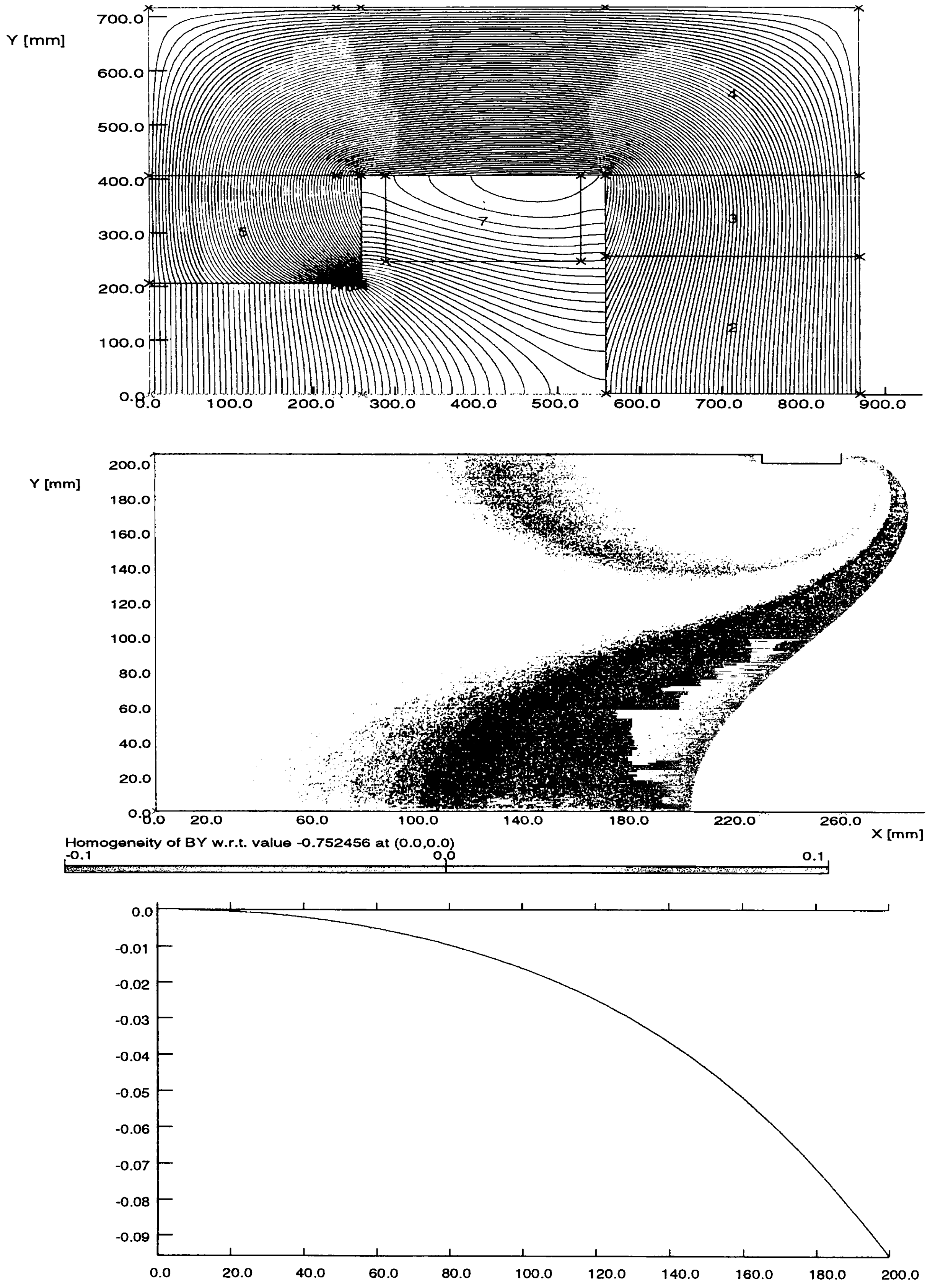

Figure 6: Magnetic properties of the M200-type magnet to be used as sweeping magnet for the TOF Facility with 410 mm gap. The field lines are shown in the upper part. In the centre part the contour plot of the field distribution in the magnet gap is plotted. Finally, in the lower part the field homogeneity is presented.

Type	2 meter bending magnet straight poles
Pole facc [mm^2]	2000 × 520
Gap height [mm]	110, 140 (nominal) 170, 200
Bending power [T m]	3.63
Resistance at 20° C [Ω]	0.195
Max. temperature	40° C at inlet and 80° C at outlet
Max. power	140 kW
Water flow	66 l/min
Weight of magnet and base [Kg]	30000 6000

Table 1: Main parameters of the M200-type magnet.

with numerical simulations. For this reason, the possibility of modifying the shims in order to improve the field quality has not been taken into account.

An important point is that such a magnet has been already installed in regions with a high degree of radioactivity (primary areas of the East Hall). However, one should keep in mind that the weak point, as far as radiation hardness is concerned, is the resin used for the magnet coils. Typical values of integrated doses sustainable by the resins used to build coils are of the order of 5×10^7 Gy citeyelrep.

The water cooling should pose no problems, the water supply being taken form the TT2 tunnel [7]. The power dissipated by the magnet during normal operation, requires the presence of a ventilation system in the TT2A tunnel, in order to avoid a temperature rise in the whole tunnel. This issue will be looked up in details by the experts of the ST/CV group, but preliminary discussions allow to state that a solution to this problem exists.

Finally, it has to be mentioned that also the power converter can be recuperated from the PS stock [9].

4 Conclusions

The results presented in the previous sections lead to the conclusion that the best solution for the sweeping magnet of the TOF Facility consists in a classical electromagnet. In particular it is proposed to use an M200-type magnet. Such a device is available in the PS stock, as well as the power converter. However, it is important to stress that a number of modifications have to be foreseen, namely

- new spacing plates have to be designed and built;
- new bolts have to be built;
- the modified magnet should be tested in order to measure the magnetic properties;
- the water cooling system should be tested under similar conditions as those present in the TT2A tunnel to verify the its efficiency and the temperature increase during routine operation.

5 Acknowledgements

I would like to thank D. Cornuet, J. Delaprison and L. Durieu for many fruitful discussions and for their precious help. Furthermore, I would like to thank A. Ferrari and E. Radermaker for providing me some key parameters for the study presented in this Note.

References

[1] The TOF Collaboration, “Proposal for a Neutron Time Of Flight Facility”, *CERN SPSC* **99-8 - P 310** (1999).

[2] S. Andriamonje et al., “Feasibility Study of a Neutron TOF Facility at the CERN-PS”, *CERN PS (CA)* **98-065** (1998).

[3] A. Ferrari, private communication, (1999).

[4] G. Foster et al., in *Proceedings of 6th European Particle Accelerator Conference*, edited by J. Poole, C. Petit-Jean-Genaz (Institute of Physics - UK, London, 1998) p. 189.

[5] D. Cornuet, private communication, (1999).

[6] B. Langeseth, G. Pluym, B. de Raad, “Magnetic Measurements on the Bending Magnets of the Beam Transport System of the CERN PS”, *PS Int. (EA)* **60-14** (1960).

[7] L. Durieu, private communication, (1999).

[8] A. Fontaine, H. Schönbacher, M. Tavlet, *CERN* **98-01** (1998).

[9] J. Buttkus, private communication, (1999).

Distribution List

R. Cappi	PS/CA
D. Cornuet	SL/MS
L. Durieu	PS/CA
M. Giovannozzi	PS/CA
M. Martini	PS/CA
D. Möhl	PS/DI
E. Radermacher	EP/DI
J-P. Riunaud	PS/CA
M. Sassowsky	SL/MS
K. Schindl	PS/DI
D-J. Simon	PS/DI